

DC electrical stimulation for chronic wound healing enhancement. Part 2. Parameter determination by numerical modelling

Dejan Šemrov^{*}, Renata Karba, Vojko Valenčič

Faculty of Electrical Engineering, University of Ljubljana, Tržaška 25, 1000 Ljubljana, Slovenia

Abstract

A three dimensional finite element model of the cutaneous wound stimulated by direct electric current was built by means of the finite element method. As was assumed in part 1 of this article, the endogenous electrical properties of the injured skin are beneficial and necessary for a normal course of healing. Therefore, an attempt was made to determine the parameters of transcutaneous electrical stimulation which would result in an electric field similar to the endogenous one in the wound area. The main goal of the study was to evaluate the influence of the electrodes' shape, size and position on the distribution of electric field in the epidermal layer at the edge of the injured tissue. The wound and the surrounding tissues were modelled as a cylinder with the spherical shaped cut-off representing the wound. 5 layers of the skin and subcutaneous tissues were modelled: epidermis, dermis, subcutis, and deeper lying fat and muscle tissue. In the parametric study performed, the influence of different electrode configurations on the distribution of the electric field was studied. Different sizes and positions of electrodes were examined by applying appropriate boundary conditions. Electric field distributions were calculated for each case and the differences in the resulting electric field were examined. According to the results obtained, some guidelines are given for the selection of the electrodes configuration in the DC electrical stimulation for chronic wound healing enhancement. © 1997 Elsevier Science S.A.

Keywords: Electrical stimulation; Direct current; Wound healing; Numerical modelling; Finite element method; Electric field distribution

1. Introduction

The clinical study, which was described in Part 1 of this series [19], showed that the effectiveness of the chronic wound healing, enhanced by DC electric current, significantly depends on the electrode configuration used. The results are not surprising if we consider differences in the electric field distributions calculated for different electrode configurations. Differences obtained for the two electrode configurations discussed lead to further analysis and optimisation of the parameters of DC electrical stimulation (shape, position and size of the stimulating electrodes). This is very difficult to perform in a clinical study since it would require a lot of time and is also questionable from the ethical point of view. Numerical modelling is an efficient and relatively inexpensive tool to perform such analysis and optimisation. The influence of different stimu-

lation parameters can easily be examined and the distribution of the electric field inside the tissue can be observed throughout the entire model.

Most of the numerical techniques allow for the definition of arbitrary geometry, material properties and boundary conditions. Analytical methods, on the other hand, usually require model characteristics to be expressed as simple analytic expressions in the chosen co-ordinate system, i.e. Cartesian, spherical or cylindrical. Those models, in which this condition is not fulfilled result in complicated systems of equations, which are difficult to solve. Complex geometries, inhomogenities and anisotropies of the tissue properties are characteristic of most biological systems. The use of numerical techniques would therefore be more appropriate in such studies. The finite element method [1] has proven to be very effective in numerous computations of the electric field inside biological systems [2–9]. In our study, the finite element method was used to calculate the electric field in a three dimensional model of the cutaneous wound stimulated by a weak direct electric current.

^{*} Corresponding author. Tel.: +386 61 1768264; fax: +386 61 1232278; e-mail: dejan@svarun.fe.uni-lj.

As was assumed in Part 1 of this series [19], endogenous epidermal battery and resulting injury currents are beneficial and necessary for a normal course of cutaneous wound healing. Therefore, we can conclude that the optimal electric field distribution, resulting from transcutaneous electrical stimulation, will be very similar to the endogenous one. A parametric study on the model was performed using this criterion. The main goal of the study was to evaluate the influence of the electrodes' position, size and shape on the distribution of electric field in the epidermal layer at the edge of the injured tissue. Electric field distributions for different electrode configurations were compared in order to find a configuration which would produce an electric field similar to the endogenous one. Finally, some guidelines for the selection of the stimulation electrodes' shape and position are suggested.

2. Materials and methods

The electric field in the biological tissue, resulting from constant direct electric current stimulation, can be treated as quasi-stationary, i.e. its time variations need not be considered. It is described by equations for the steady electric currents in the volume conductor. If the resistivity of the volume conductor is homogenous and isotropic, then the electric potential distribution is governed by the Laplace equation. Two types of boundary conditions apply in this situation. A Dirichlet boundary condition is represented as a fixed scalar electric potential, i.e. applied voltage on the surface of the model. A Neumann boundary condition is represented as a first derivative of the scalar electric potential in the direction normal to the boundary surface of the model, i.e. current density flowing in/out of the model multiplied by the resistivity of the tissue.

2.1. Geometry definition

A three dimensional finite element model of the cutaneous wound stimulated by direct electric current was built using MSC/EMAS (electromagnetic analysis system) software package (trademark of MacNeal–Schwendler) [10–12]. The geometry and finite element mesh definition, as well as plotting of the results, was performed using the MSC/XL software package, while matrix solving was done by MSC/EMAS. The wound and the surrounding tissue were modelled as a cylinder with the spherical shaped cut-off representing wound. The diameter of the model (cylinder) was 180 mm and its height was 13.5 mm. The diameter of wound was 60 mm, and its depth was 4 mm. Five layers of skin and subcutaneous tissues were modelled: epidermis, dermis, subcutis and deeper lying fat and muscle tissue. We assumed that no electric current is flowing through the underlying bone, since its electric resistivity is high compared to the resistivity of muscle tissue. Therefore, we applied the appropriate boundary

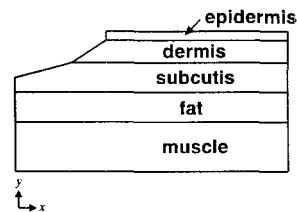


Fig. 1. One half of the cross-section of the three-dimensional geometry of the wound model. The region above the upper left part represents the wound area.

condition in the boundary surface between muscle and bone so that the normal derivative of the electric potential was set to 0. The thickness of epidermis was 0.3 mm, dermis 2.2 mm, subcutis 3 mm, fat 3 mm, and muscle tissue 5 mm. In Fig. 1, one half of the cross section of the model is shown. By rotating this geometry around the y-axis by 360°, a three dimensional model of the wound and surrounding tissue is obtained.

2.2. Mesh generation

Since the geometry of the model is axisymmetric, finite element mesh was first generated using two-dimensional finite elements on the half of the cross section presented in Fig. 1. Quadrilateral elements were used in all layers of the model and the appropriate tissue label was assigned to each element. Muscle tissue was modelled with 50 finite elements. Fat and connective tissue layers were modelled with 75 finite elements each. In the layer representing dermis a mesh of 39 finite elements was generated, while the epidermal layer consisted of 10 finite elements. This mesh was then rotated around the y-axis by 360° and a three dimensional finite element mesh was built. This is presented in Fig. 2 together with the cross section in which the resulting electric field distribution was observed. Highlighted is a part of the cross section in which the results are presented in Figs. 4–7. The model contained elements with 6 boundary surfaces (resembling bricks) and elements with 5 boundary surfaces (resembling wedges) in the region near the axis of rotation. The density of the elements in the two dimensional mesh was higher towards the axis of rotation in order to obtain a more regular (cube like) shape of the elements. The rotation was made in 24 steps, 15° each. The mesh was made up of 6120 three-dimensional finite elements which yielded 6753 grid points where computation of the scalar electric potential was performed. Distributions of electric field strength were then calculated from the potential distribution.

2.3. Tissue characteristics

The electric resistivity values were collected from the literature [13–18]. 5 layers of the skin and subcutaneous tissue were modelled as homogenous, isotropic materials. We did not consider the fact that epidermis and dermis are

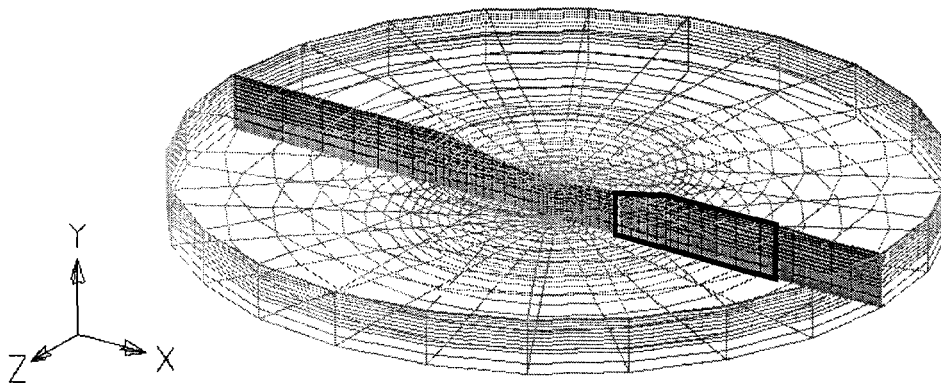


Fig. 2. Finite element model of the wound with cross-section plane in which the distribution of the resulting electric field was observed.

polarised epithelia and we also neglected the influence of Na/K pumps on the basal membrane of each layer on the resulting electric field distributions. Namely, what we were most interested in was the influence of the electrodes' shape, size and position on the distribution of the electric field resulting from external electrical stimulation. The electric fields resulting from the above mentioned endogenous electrical phenomena in the tissue are simply added to the electric fields resulting from external electrical stimulation that were the main object of our study. The more realistic model would then be a combination of the proposed model and the model of endogenous electrical phenomena.

The selected electric resistivity values were assigned to appropriate finite elements before the computation was performed. The average resistivity was determined for the whole epidermis, although substantial differences in resistivities with respect to the distance from the skin surface were reported [14]. For the outermost layer of the epidermis, i.e. the stratum corneum, we selected the lowest value of resistivity ($250 \Omega \text{ m}$) from the values reported in the same reference, which is typical for the innermost edge of the stratum corneum. Namely, during the standard wound care treatment the outermost extremely high resistive keratinized horny layer of the normal skin surrounding the wound is constantly removed by cleaning and disinfection. The result of this is lower resistivity of the outermost region in the case of pressure ulcers treated in the clinical study, which was also selected in our model. For the deeper layers of epidermis, i.e. stratum lucidum, stratum granulosum, stratum spinosum and stratum basale, we chose lower resistivity ($4.5 \Omega \text{ m}$), as suggested in [14]. The average resistivity of the whole epidermis was then determined with respect to the thickness of the corresponding layers, and its value was $38.5 \Omega \text{ m}$. The same resistivity as for deeper layers of epidermis ($4.5 \Omega \text{ m}$) was chosen for dermis. The resistivity of the whole skin (dermis and epidermis together) was then $8.3 \Omega \text{ m}$. The resistivity of the subcutis (connective tissue) was determined as an average between the resistivities of the skin ($8.3 \Omega \text{ m}$) and deeper lying fat ($21.7 \Omega \text{ m}$, [17]), and its value was 12.5Ω

m. Although the anisotropic character of the muscle tissue is reported in most of the references [13,15–18], we did not consider this feature since in our study we concentrated on the influence of the electrode configuration on the electric field distribution in the skin layers. Therefore, an average value of $2.2 \Omega \text{ m}$ was selected.

The sensitivity of the resulting electric field to the choice of the electric resistivity values was not examined since we were interested only in the geometry, position and dimensions of the electrodes. However, a selection of other electric resistivity values can produce a significant change in the results. The influence of these parameters needs to be analysed in one of next studies.

2.4. Boundary conditions — electrode configuration

Different shapes and sizes of the electrodes were examined by applying appropriate boundary conditions in the grid points on the surface of the model. Both types of boundary conditions were applied. Fixed values of the scalar electric potential, i.e. Dirichlet boundary conditions, were assigned to selected grid points in the regions where electrodes were placed. Their geometries need not to be rotational symmetric as was the finite element mesh, since the software used enables any boundary condition geometry be defined. This was applied in the DC + and DC \pm configurations in Part 1 of this series [19] and also justified the selection of the three dimensional finite element model for this study. In the case of the complete rotational symmetry, where the geometry, material characteristics and boundary conditions are all rotational symmetric, a two dimensional axisymmetric finite element model would suffice for the solution of the problem. In all the remaining regions of the outer boundary surface of the model, a Neumann boundary condition was applied. It was required that no current be flowing in/out of the model in the direction perpendicular to the outer surface of the model since the resistivity of the air surrounding the model is much higher than the resistivity of all tissues modelled. Therefore the value of the electric current density in the normal direction was chosen to be 0 A m^{-2} in all bound-

ary regions of the model where fixed electric potential was not applied.

In the parametric study the influence of the electrodes' position, size and shape on the distribution of electric field in the epidermal layer at the edge of the injured tissue was examined. According to the results of the clinical study and modelling reported in Part 1 of this series [19], two different shapes were selected for positive and negative electrode. The first was ring-shaped, and was placed on the healthy skin surrounding the wound, while the second was circular and placed on the surface of the wound. Their dimensions and positions were varied. The potential of 0 V was assigned to the ring-shaped electrode on the uninjured skin, and the appropriate positive scalar electric potential was assigned to the circular electrode on the wound surface, so that the total current flowing in/out of the model was 0.6 mA. This current was delivered to the wound from the electrical stimulator working in current source mode in the clinical study, described in Part 1 of this series [19]. The top view for the four electrode configurations examined is shown in Fig. 3. In configuration 1, the width of the ring-shaped electrode was 40 mm and it reached the edge of the wound. The circular electrode covered the whole open surface of the wound, i.e. outer surface of the subcutis and dermis up to the lower edge of epidermis, and the potential of 13 mV was assigned to the corresponding grid points. In configuration 2, the width of the ring-shaped electrode was 20 mm and the distance between its inner edge and the edge of the wound area was 20 mm. The circular electrode covered only the outer surface of the subcutis, and the potential of 76 mV was assigned to the corresponding grid points. In configurations 3 and 4, the combinations of electrodes applied in configurations 1 and 2 were used. In configuration 3, the dimensions and position of the ring-shaped electrode covering uninjured skin was the same as in configuration 2, i.e. its width was 20 mm and its inner edge was 20 mm from the wound edge. The circular electrode covered the whole area of the wound as in configuration 1, and the potential of 39 mV

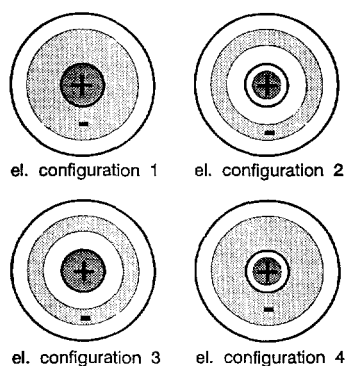


Fig. 3. Electrode configurations examined in the study. The ring-shaped electrode (negative) was placed on the normal skin surrounding the wound. The circular electrode (positive) was placed on the surface of the wound.

was assigned to the corresponding grid points. In configuration 4 the ring-shaped electrode was the same as in configuration 1, i.e. 40 mm wide and covered healthy skin up to the wound edge, while the circular electrode covered only the outer surface of subcutis as in configuration 2, and the potential of 61 mV was assigned to the corresponding grid points.

3. Results

Distributions of scalar electric potential were determined inside the model for four different electrode configurations. Distributions of other electric quantities were then calculated from the values of the scalar electric potential in the grid points of the model. Electric field distributions were observed in the cross section plane through the middle of the model, since we were most interested in the electrical phenomena inside tissue. They were then compared to the electric field calculated in the model of endogenous electrical phenomena (epidermal battery), presented in Part 1 of this series [19]. That field was homogenous with the magnitude of electric field strength of 1 V cm^{-1} and directed from the lower to the upper edge of epidermis.

In Figs. 4–7 the results for electrode configurations 1, 2, 3 and 4 are presented, respectively. The meshes represent the cross section of the 3D finite elements in the selected part of the model as shown in Fig. 2. The axes at the bottom of each plot represent the orientation of the cross section with respect to the whole model. This orientation was the same for all plots. On the left side of each figure, the magnitude of electric field strength is presented. The patches with different intensity of shading inside the meshes represent appropriate values of magnitudes of electric field strength in the corresponding region of the model. The legend above defines the intervals of electric field strength that are represented by the appropriate intensity of shading. The scale used was logarithmic and it was the same as in the results presented in Part 1 of this series [19]. On the right side of each figure the direction of the electric field strength in the same part of the model can be observed. Arrows represent vectors of electric field strength for the corresponding finite elements. The length of each arrow is proportional to the magnitude of the electric field strength inside each particular finite element. The reason for the discrepancy between the length of arrows in the right plot and shading in the left plot in some figures is the averaging of the results which is performed when contour plots (left) are calculated. This averaging is used to get smoother transition of the electric field strength magnitude between particular finite elements which is closer to the real electric field distribution. Namely electric field strength is calculated for each particular finite element and is constant inside it. As a result of this, electric field strength

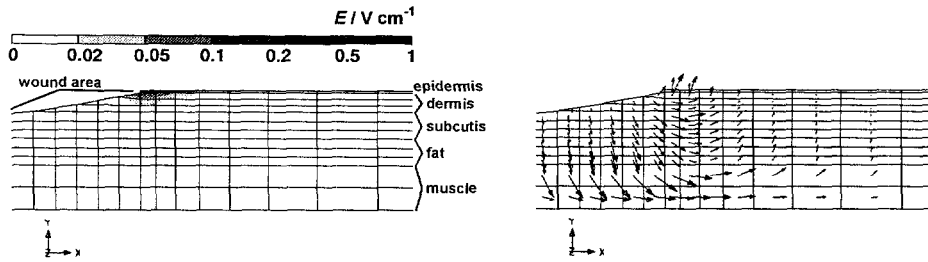


Fig. 4. Electric field distribution for electrode configuration 1. The electric field in the epidermis near the edge of the wound is most similar to the endogenous, reported in Part 1 of this series [19].

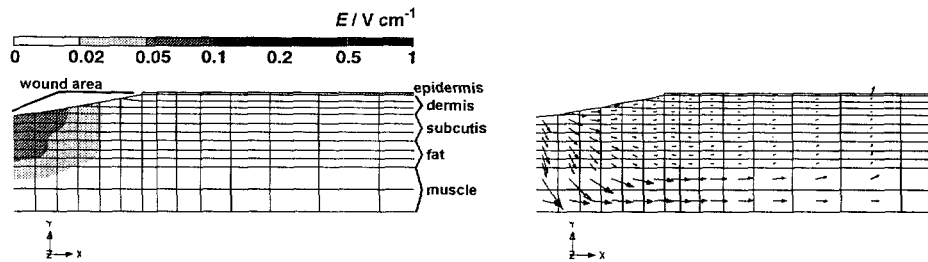


Fig. 5. Electric field distribution for electrode configuration 2. This configuration was the least appropriate as regards similarity to the endogenous electrical phenomena.

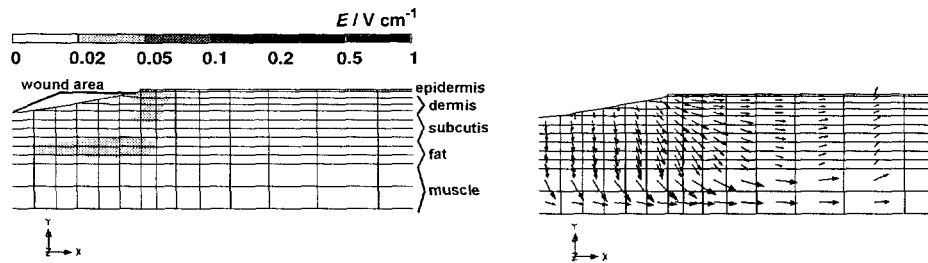


Fig. 6. Electric field distribution for electrode configuration 3. This configuration is the worst compromise between the electrode configurations 1 and 2.

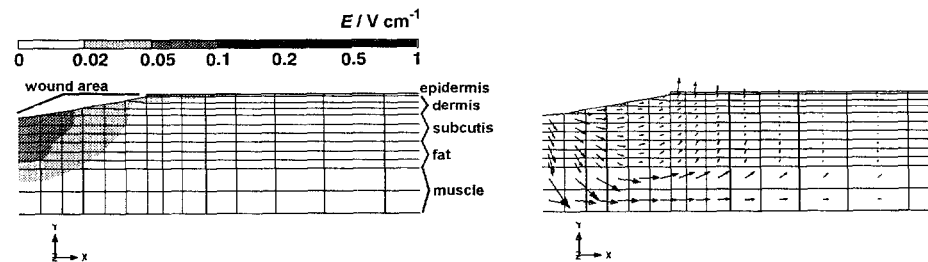


Fig. 7. Electric field distribution for electrode configuration 4. This configuration is the best compromise and suitable for implementation in practice.

transition between finite elements is discrete, which is not in accordance with the realistic situation. To avoid that and obtain smooth transitions, averaging is performed.

Fig. 4 shows the results for electrode configuration 1. The magnitude of the electric field strength reaches its maximum in the epidermal layer near the edge of the wound, and its value is 0.28 V cm^{-1} , which is approximately one quarter of the electric field strength resulting from the epidermal battery. The direction of the electric field, shown on the right side, is also similar to the direction of the endogenous electric field presented in Part 1 of this series [19]. This electrode configuration is thus the most appropriate according to the criteria selected for our study, i.e. the agreement of externally induced electric field with the endogenous situation.

Distribution of the resulting field for electrode configuration 2 is shown in Fig. 5. The region of the maximal magnitude of electric field strength is located in layers below the wound surface, away from the epidermal layer. The direction of the electric field in the epidermis near the wound edge is perpendicular to the desired direction, as obtained in the model of endogenous electrical phenomena. The magnitude of the electric field strength in the epidermis near the edge of the wound is 0.01 V cm^{-1} , which is 100 times lower than in the model of the endogenous field.

Distribution of the resulting field for electrode configuration 3 is shown in Fig. 6. In the epidermis, the magnitude of the electric field strength is slightly higher (0.038 V cm^{-1}) than for electrode configuration 2, but its direction is even more different from the desired direction, typical of the endogenous field.

The distribution of electric field for the electrode configuration 4 is shown in Fig. 7. The region of the maximal electric field strength magnitude is again moved to the lower edge of the model. However, there is a substantial rise in electric field strength in the epidermal layer with the magnitude of 0.13 V cm^{-1} , which is still 10 times lower than in the model of endogenous electric field. Its direction is quite similar to the direction obtained in the model of the epidermal battery.

A summary of results for the magnitude of the electric field strength in the epidermis on the edge of the wound for different electrode configurations is listed in Table 1.

Table 1
Magnitudes of electric field strength in the epidermis on the edge of the wound

Electrode configuration ^a	$ E \text{ (V cm}^{-1}\text{)}$
1	0.28
2	0.01
3	0.038
4	0.13

^a Described in materials and methods section and shown in Fig. 3.

4. Discussion

Finite element modelling has proven to be an efficient tool in our parametric study, where the influence of the electrodes' shape, size and position on the distribution of electric field inside the model of the chronic wound stimulated by direct electric current was examined.

As was shown in Part 1 of this series [19], the epidermal battery, i.e. the difference in ionic concentrations between the upper and the lower edge of epidermis, results in a homogenous electric field in the epidermal layer. The direction of the electric field strength is from the lower to the upper edge of the epidermis and its magnitude is 1 V cm^{-1} . This result serves as confirmation of the method and of the model, since it agrees with the simple analytical calculation of the electric field between two charged plates of the ideal electric capacitor.

When different shapes, sizes and positions of the transcutaneous electrodes are concerned, analytical calculation does not suffice. As had been expected, direct electric current stimulation with the ring shaped negative electrode placed on the uninjured skin around the wound, and circular positive electrode covering the open surface of the wound, results in an electric field quite similar to the endogenous one. However, the position and size of the electrodes substantially influence the distribution of the electric field strength inside the model. The best accordance with the endogenous electric field is obtained when the ring-shaped electrode covers the surrounding healthy skin up to the edge of the wound and the circular electrode covers the whole outer surface of the wound (dermis and subcutis) up to the lower edge of the epidermis (configuration 1). The resulting field is similar to the endogenous electric field in direction, and the magnitude of electric field strength has a maximum of 0.28 V cm^{-1} in the epidermal layer near the edge of the wound. However, this electrode configuration is very difficult to implement in clinical wound care, especially if the circular electrode is required exactly to reach the lower edge of epidermis.

Configuration 2 represents the opposite (worst) extreme, where neither the ring-shaped nor the circular electrode reaches the upper or lower edge of the epidermal layer. The magnitude of the electric field strength in the epidermal layer (0.01 V cm^{-1}) is the least of all configurations, and its direction considerably differs from the endogenous one in the epidermis near the edge of the wound.

The resulting fields for the intermediate electrode configurations 3 and 4 were rather different from each other. Configuration 3 resulted in an electric field similar to the one obtained with configuration 2, but again quite different from the one desired, typical for endogenous electrical phenomena. The magnitude of the electric field strength in the epidermis near the edge of the wound (0.038 V cm^{-1}) was slightly higher than in the model with electrode configuration 2 (worst extreme), and its direction was even more unsuitable. Much better results were obtained with

configuration 4, where the ring-shaped electrode covered healthy skin up to the wound edge, while the circular electrode covered only the outer surface of the subcutis. The magnitude of electric field strength had a rise in the epidermal layer near the edge of the wound, and its value was 0.13 V cm^{-1} . Its direction is in good agreement with the desired direction of the field resulting from epidermal battery. Configuration 4 is therefore the best compromise.

According to the results obtained, some guidelines for the electrode geometry, size and position can be offered for the direct current transcutaneous electrical stimulation of chronic wounds, if maximal similarity to the endogenous electric field in the epidermis is desired. The negative electrode should be placed on the healthy skin around the wound. It should be surrounding the wound area, and it is essential that it comes as close as possible to the wound edge. The positive electrode should be placed directly on the open surface of the wound and, although it is not essential that it reaches the lower edge of epidermis, it is still recommendable that it covers a major part of the wound surface. These requirements are not too difficult to meet in clinical applications of DC stimulation for wound healing enhancement, and all conclusions mentioned above should be checked in further clinical studies.

Acknowledgements

This research was supported by the Ministry of Science and Technology of the Republic of Slovenia.

References

- [1] O.C. Zienkiewicz, *The Finite Element Method* (McGraw-Hill, London, 1977).
- [2] N.G. Sepulveda, C.F. Walker and R.G. Heath, *J. Biomed. Eng.* 5 (1983) 41.
- [3] Y. Kim, J.B. Fahy and B.J. Tupper, *IEEE Trans. Biomed. Eng.* (1986) 845.
- [4] J.B. Fahy, Y. Kim and A. Ananthaswamy, *IEEE Trans. Biomed. Eng.* 34 (1987) 743.
- [5] K.P. Kothiyal, B. Shankar, L.J. Fogelson and N.V. Thakor, *Proc. IEEE* 76 (1988) 720.
- [6] E.L. Carter, E.J. Vresilovic, S.R. Pollack and C.T. Brighton, *IEEE Trans. Biomed. Eng.* 36 (1989) 333.
- [7] N.G. Sepulveda, J.P. Wiskwo and D.S. Echt, *IEEE Trans. Biomed. Eng.* 37 (1990) 354.
- [8] E.L. Carter, S.R. Pollack and C.T. Brighton, *IEEE Trans. Biomed. Eng.* 37 (1990) 606.
- [9] S.S. Nathan, S.R. Sinha, B. Gordon, R.P. Lesser and N.V. Thakor, *Electroenceph. Clin. Neurophys.* 86 (1993) 183.
- [10] J.R. Brauer and B.E. MacNeal (Eds.), *MSC/EMAS User's Manual Version 2.5* (MacNeal-Schwendler Los Angeles, 1991).
- [11] B.E. MacNeal (Ed.), *MSC/EMAS Modelling Guide* (MacNeal-Schwendler, Los Angeles, 1993).
- [12] K.H. Peterson (Ed.), *MSC/XL User's Manual Version 3A* (MacNeal-Schwendler, Los Angeles, 1992).
- [13] H.P. Schwan and C.F. Kay, *Ann. NY Acad. Sci.* 65 (1957) 1007.
- [14] T. Yamamoto and Y. Yamamoto, *Med. Biol. Eng.* (1976) 151.
- [15] H.C. Burger and R. van Dongen, *Phys. Med. Biol.* 5 (1960–61) 431.
- [16] S. Rush, J.A. Abildskov and R. McFee, *Circul. Res.* 12 (1963) 40.
- [17] L.A. Geddes and L.E. Baker, *Med. Biol. Eng.* 5 (1967) 271.
- [18] H.P. Schwan and K.R. Foster, *Proc. IEEE* 68 (1980) 104.
- [19] R. Karba, D. Šemrov, L. Vodovnik, H. Benko and R. Šavrin, *Bioelectrochem. Bioenergy.* 43 (1997) 265.